

Cite this: *Org. Biomol. Chem.*, 2023, **21**, 3525Received 28th March 2023,
Accepted 11th April 2023

DOI: 10.1039/d3ob00473b

rsc.li/obc

Combining local conformational preferences and solvophobic effects in helical aromatic oligoamide foldamers†

Binhao Teng,^a Joan Atcher,^a Lars Allmendinger,^a Céline Douat,^b Yann Ferrand^b and Ivan Huc^{a*}

Aromatic oligoamide foldamers were designed using a newly-developed monomer so that helical folding was promoted by both local conformational preferences and solvophobic effects. Solid phase synthesis provided quick access to the desired sequences. Sharp solvent-driven conformational transitions that depended on sequence length were evidenced by both NMR and UV absorption spectroscopies.

Aromatic foldamers constitute a large ensemble of oligomers with aryl rings in their main chain that have stable folded conformations, most frequently helices. Helical folding may be driven by multiple parameters including solvophobic effects,^{1–7,9} the presence of neutral or ionic guests,^{10–14} steric congestion combined with aryl–aryl interactions,^{15,16} or local conformational preferences.^{17–21} The latter are typically mediated by hydrogen bonds and electrostatic repulsions between adjacent aryl rings or between aryl rings and amide groups, eventually restricting single bond rotations. In their absence, folding is altered.²² Conversely, folding may be so strongly driven by local conformational preferences that it occurs in essentially any solvent.²³ The solvent then simply modulates helix stability, but neither unfolding nor important conformational transitions are observed. A benefit of high conformational stability is that it enhances crystal growth ability for the purpose of solid-state structure elucidation. In contrast, solvophobic foldamers have rarely been crystallized. Several approaches using hydrogen bonds or polar interactions have been proposed to reinforce the helical structures of solvophobic aromatic foldamers.^{24–29} Here, we present an opposite strategy consisting in deliberately decreasing conformation control by removing some local conformational preferences

from helical aromatic oligoamide foldamers (AOFs), while at the same time allowing for a larger role of solvophobic effects. The main motivation was to elicit and investigate conformational transitions in objects that would otherwise be rigid. Conformational transitions enrich structural behavior and allow, for example, for the dynamic control of properties such as anion recognition or self-assembly.^{30,31}

Q and Q^F are typical monomers of AOF sequences in which helical folding is driven by local conformational preferences (Fig. 1).^{17,23,32,33} In such AOFs, quinine endocyclic nitrogen atoms or exocyclic fluorine atoms form hydrogen bonds with amide protons and concomitantly engage in repulsive electrostatic interactions with amide carbonyl groups. In contrast, the new 7-amino-2-quinolinecarboxylic acid monomer Q^H also has an endocyclic nitrogen atom, but no function adjacent to its 7-amino group that could set the orientation of an amide at that position. Pseudo-conjugation is therefore expected to favor two *s-cis* and *s-trans* conformers in which the quinoline

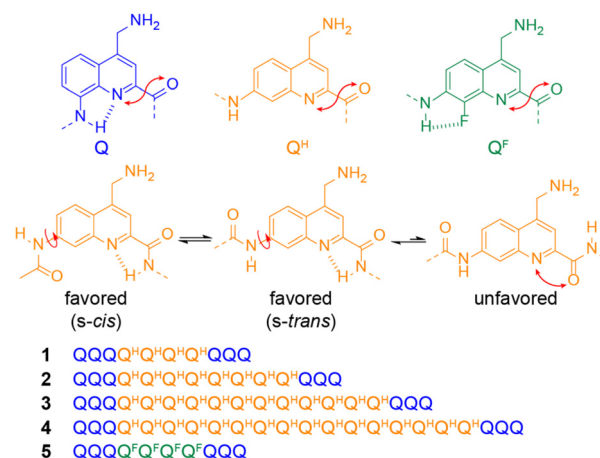


Fig. 1 Structures of color-coded monomers Q, Q^H and Q^F and composition of sequences 1–5. When placed in an AOF sequence, Q^H may adopt two main conformations. Double-headed arrows indicate electrostatic repulsions.

^aDepartment of Pharmacy, Ludwig-Maximilians-Universität, Butenandstr. 5–13, 81377 München, Germany. E-mail: ivan.huc@cup.lmu.de

^bUniv. Bordeaux, CNRS, Bordeaux Institut National Polytechnique, CBMN UMR 5248, 2 rue Escarpite, 33600 Pessac, France

† Electronic supplementary information (ESI) available: Synthetic protocols and characterisation of new compounds. See DOI: <https://doi.org/10.1039/d3ob00473b>

ring of Q^H and adjacent amide groups are coplanar, leading to 2^n conformers in a sequence having n Q^H units (Fig. 1).

For this study, monomers Q , Q^H and Q^F were all equipped with a 4-aminomethyl group which, once protonated, ensures good water solubility of AOF sequences. The choice of this small polar side chain was also made in the hope it would favor crystal growth.³⁵ Monomer Q has previously been described,³⁵ yet an improved synthesis is presented in the ESI (ESI, Scheme S1†). The syntheses of monomer Q^F which had never been presented with this side chain and of new monomer Q^H are also shown in the ESI (Schemes S2 and S3†). All were produced on a 10 g scale as building blocks ready for solid phase synthesis (SPS), that is, with a free carboxylic acid in position 2, and their main chain and side chain amines protected with Fmoc and Boc, respectively.

We designed sequences 1–4 to investigate the folding behavior of Q^H monomers (Fig. 1). These sequences contain Q_4^H , Q_8^H , Q_{12}^H , or Q_{16}^H segments. Sequence 5 is analogous to 1 with Q^F units instead of Q^H . The importance of assessing any length dependence in such studies has been highlighted by Moore *et al.*⁸ and we thus headed for a series instead of a single compound. Energy-minimized models show that it takes about 4.5 Q^H units to span one turn when this monomer is involved in a helix (Fig. 2a–d). In their helical conformations, the Q_n^H segments of 1–4 would thus be expected to

span about 0.9, 1.8, 2.7 or 3.6 helix turns, respectively. Our expectation was that water may favor the helical conformations of 1–4 because these conformations reduce the solvent exposure of Q^H monomers. However, this may not occur in solvents that solvate the aryl amide groups such as DMSO where the Q_n^H segments may adopt any conformations from the helix (with 7-amido-quinoline bonds all in *s-trans*) to a fully extended form (Fig. 2e, with 7-amido-quinoline bonds all in *s-cis*). As an illustration, the solvent exposed surface of 2 in its helical and fully extended Q_8^H conformations were calculated to be 1720 and 2580 Å², respectively, giving a measure of how much is hidden from the solvent upon helix folding (Fig. S1†).

Q_n^F analogues bearing other side chains have a strong propensity to aggregate into multistranded structures through a spring-like extension and intertwining of their helices, including in water.^{32,36} In anticipation that Q_n^H sequences may also aggregate and that this would complicate the investigation of their folding behavior, all sequences were flanked by Q_3 segments at both ends. Q monomers code for a narrower helix diameter than Q^F or Q^H – only 2.5 units per turn.^{17,32,33} Q_n oligomers with $n > 2$ do not form multistranded helices and have been shown, when placed at the termini, to prevent double helix formation of segments having a larger diameter.^{37,38} Thus, in their helical conformations (Fig. 2a–d), sequences 1–4 may possess a cavity potentially capable of encapsulating guest

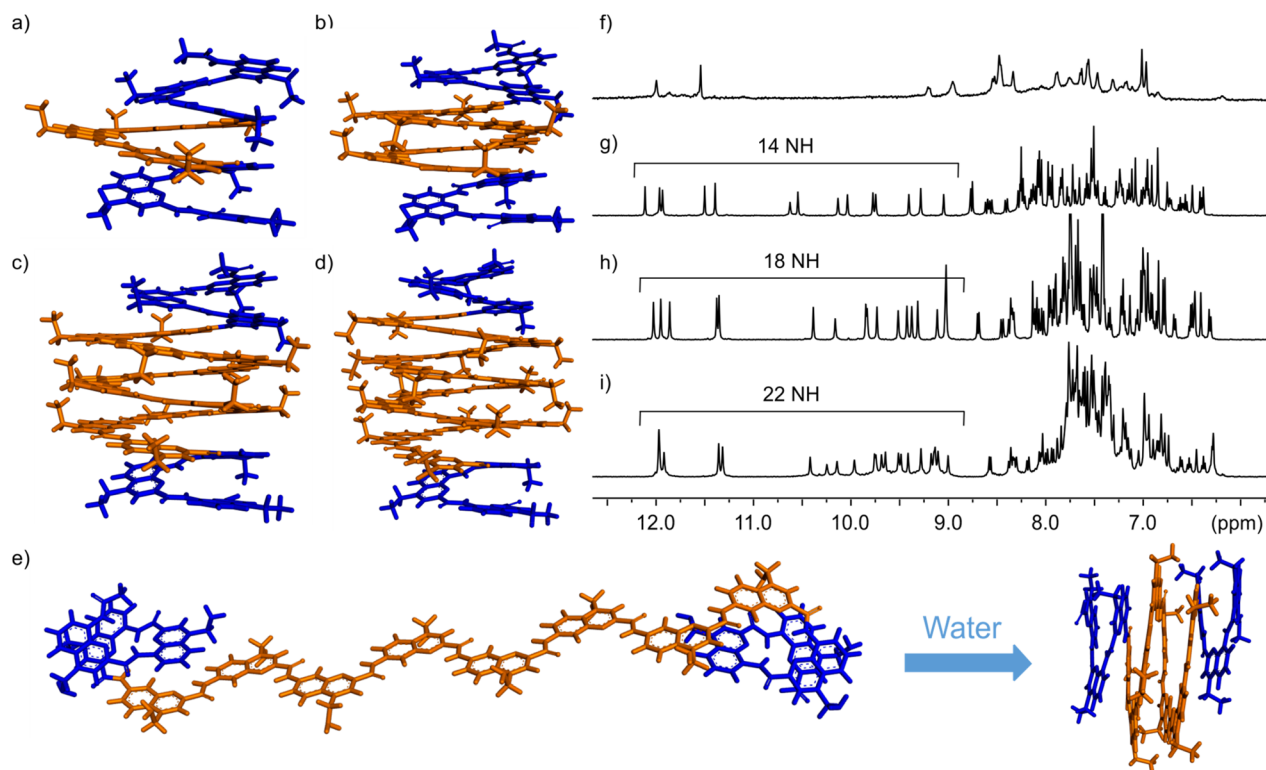


Fig. 2 Energy minimized conformations (Maestro, MMFFs force field, water as implicit solvent)³⁴ of 1 (a), 2 (b and e), 3 (c) and 4 (d). In (a–d), the Q_n^H segments have been arranged as a helix at the start of the minimization whereas in (e) it was placed in an all extended conformation. (e) thus illustrates two extreme conformational states. (f–i) Excerpts from the 500 MHz ¹H NMR spectra of compounds 1 (f), 2 (g), 3 (h), and 4 (i), all recorded at 298 K in H₂O/D₂O (90 : 10 v/v).

molecules, as in designs that we and others have presented previously.^{7,37–39} This potential was an additional motivation when designing 1–4. Yet their molecular recognition properties will be described elsewhere.

A third motivation in the design of 1–4 was to challenge the preparation of such sequences by SPS. SPS protocols are very efficient for sequences such as Q_n derivatives with various side chains,^{35,40} and have recently been automated.⁴¹ Their applicability to entire capsule-like sequences was unknown but desirable for quicker access in the context of iterative sequence improvements.^{42,43} As presented in detail in the ESI,[†] SPS proved to be very efficient, generating sequences in good crude purity and allowing for their isolation using RP-HPLC in 15–32% isolated yield. The only exception was sequence 5 which repeatedly gave poorer yields for reasons that were not identified.

The ^1H NMR spectra of 2–4 at 0.5 mM in $\text{H}_2\text{O}/\text{D}_2\text{O}$ (90 : 10 v/v) showed a single set of sharp resonances typical of folded conformations (Fig. 2g–i). In particular, distinct signals with very little overlap are clearly observed for the amide NH resonances even for the longest sequence 4. In contrast, the signals of 1 were broader (Fig. 2f), suggesting that some conformational dynamics, or some aggregation, were at play. The spectrum of 2 did not change significantly upon varying concentration, hinting at a monomeric species or a very stable aggregate (Fig. S2[†]). In $\text{DMSO}-d_6$, a solvent that inhibits the aggregation of aromatic oligoamides and that provides weaker solvophobic effects than water, one set of ^1H NMR signals is also observed for all species but the patterns of signals differ from those of water (Fig. 3). Only a limited number of distinct amide NH resonances were observed, that were assigned to the NH protons of the folded Q units. Several NH signals appear under the same large peak whose intensity correlates with the length of the central Q_n^{H} segment (Fig. 3, green circle). The spectra also tend to become broader as the length of this segment increases. This trend is consistent with the Q_n^{H} segment undergoing the *s-cis/s-trans* equilibrium shown in Fig. 1. In the absence of folding that would make their environment different due to the ring current effects associated with aromatic stacking, the NH resonances of Q_n^{H} segments have, on average, a similar chemical shift value in $\text{DMSO}-d_6$. Equilibrium between the different conformers is fast on the NMR time scale but full averaging takes more time for the longest sequences, hence the broadening of the signals.

Upon adding water to samples in $\text{DMSO}-d_6$, all four ^1H NMR spectra were found to evolve (Fig. 3). In the case of the two shorter sequences 1 and 2, an initial broadening led to a coalescence before a new set of signals emerged, indicating an equilibrium between two states that is neither fast nor slow on the NMR time scale. For the two longer sequences 3 and 4, the water-dominant species emerged before the DMSO -dominant species disappeared and co-existence of the two species in slow exchange on the NMR time scale was observed at intermediate proportions of water. These results demonstrate that, for all compounds, the prevalent species in water are different

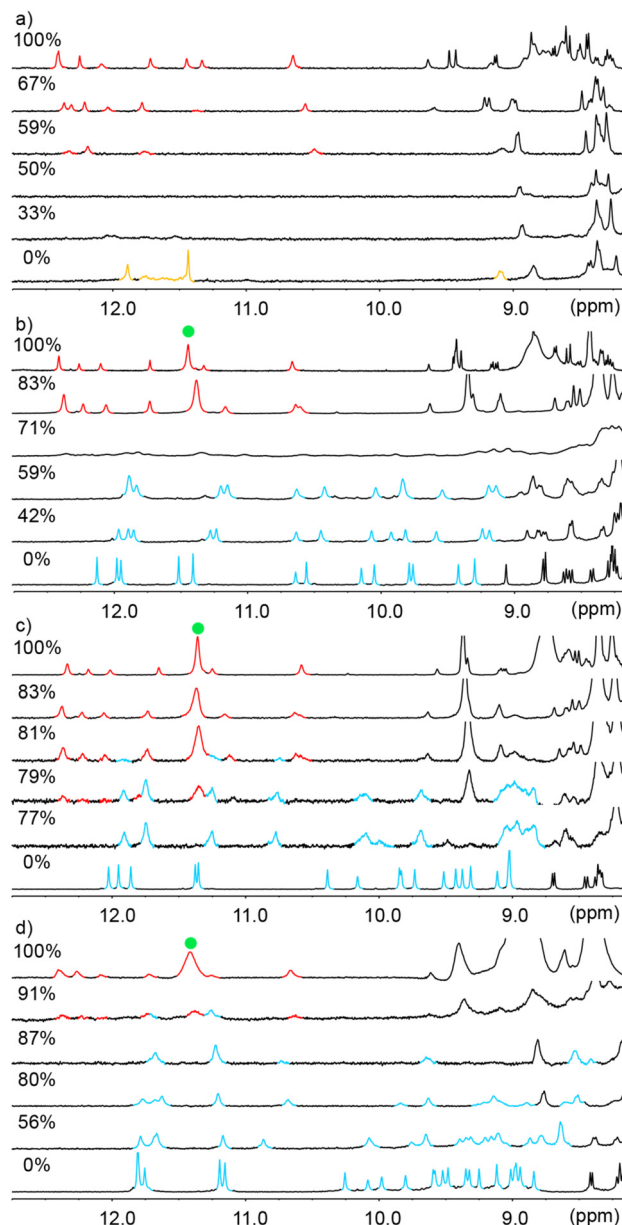


Fig. 3 Excerpts of the ^1H NMR (500 MHz) spectra of 1–4 in $\text{DMSO}-d_6/\text{H}_2\text{O}$ mixtures at 298 K. (a) 1; (b) 2; (c) 3 and (d) 4. The volume % of DMSO are indicated. Note: 0% DMSO means the spectrum was recorded in $\text{H}_2\text{O}/\text{D}_2\text{O}$ (90 : 10 v/v). Red, blue and gold color amide NH signals stand for structures in which Q_n^{H} segments adopt unfolded, helically folded and partially folded conformations, respectively. Large peaks assigned to the NH of unfolded Q^{H} units are pointed out by green circles.

from those that prevail in DMSO , and that the characteristic time of exchange between these species increases with increasing the length of Q_n^{H} segments. A similar effect was observed upon adding CD_3OH to a $\text{DMSO}-d_6$ solution of 2 (Fig. S3[†]), albeit more CD_3OH was necessary for a full transition than with water. In contrast, the NMR spectra of reference compound 5 show that it undergoes no such transition (Fig. S4[†]), as would be expected in a sequence that does not contain Q^{H} .[‡]

The water-induced transition was found to require less water as the length of the Q_n^H segment was increased (Fig. 3), suggesting some cooperative phenomena. UV spectroscopy was then utilized to further investigate this cooperative conformational transition. Fig. 4a–c shows the UV spectra of oligomers 2–4 at different proportions of water and DMSO. Increasing the water content resulted in a drop in the intensity of the band centered at 357 nm (hypochromicity), consistent with the formation of stacks of aryl rings.⁴⁴ Concomitantly, hyperchromic and hypsochromic effects were observed for the band centered at 257 nm. A decrease in the A_{357}/A_{257} absorbance ratio indicates a conformational change in water compatible with the collapse shown in Fig. 2e.⁴⁵ Most of the UV spectra cross isosbestic points, confirming an equilibrium between two states. However, at high DMSO content, the spectra no longer include the isosbestic points, indicating that more complex effects are involved (e.g. solvent dependence of the absorbance itself).

Fig. 4d depicts the relationship between the normalized UV intensity at 357 nm and the volume fraction of DMSO in water. Oligomers 2–4 with more than one helix turn at their central Q_n^H segment exhibit a sigmoidal curve characteristic of a sharp, cooperative, folding transition.⁵ The transition becomes more abrupt as the length of the chain increases. In agreement with NMR spectra, it takes less water to cause the transition of longer Q_n^H segments. The curve corresponding to **1**, shows a less clear transition that may be explained by the fact that Q_4^H is too short to span a turn. It can only undergo reduced intramolecular aromatic stacking between Q^H and Q units in its helical conformation (Fig. 2a shows two protruding, solvent exposed Q^H units). This observation is consistent with the behavior observed by NMR. The existence of a sharp folding tran-

sition induced by water suggested a possibly strong contribution of entropy and thus a dependence on temperature. We measured the UV spectra of 2–4 at temperatures ranging from 5 to 85 °C using a proportion of DMSO that was, for each compound, close to the transition point (Fig. S6–S8†). However, contrary to what has been reported for phenylacetylene oligomers,² no significant change of the UV spectra was observed.

Finally, to ascertain the structures of the folded conformations in solution, multiple attempts were made to grow single crystals. Unfortunately, the aminomethyl side chains did not serve this purpose well and no good diffracting crystals were obtained. We thus turned to NMR and managed to elucidate the structure of oligomer 2 using two-dimensional experiments (see ESI†). The spin systems of each quinoline ring were assigned using TOCSY, HBMC (e.g. correlations of H3 to the exocyclic \underline{CH}_2

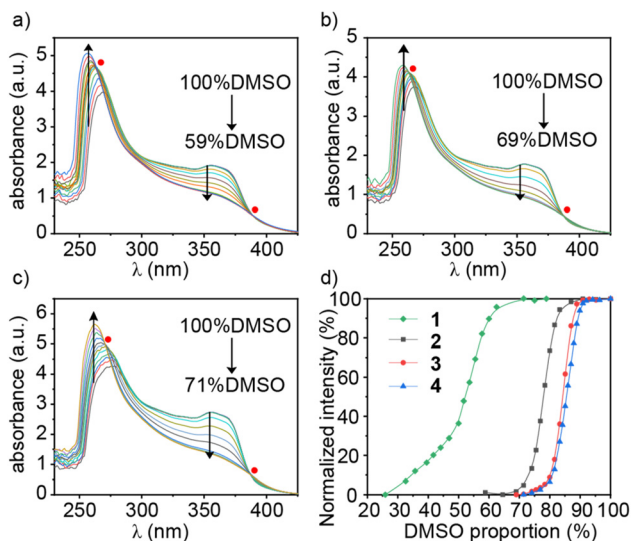


Fig. 4 UV spectra of compounds 2–4 at different proportions of water and DMSO (a–c respectively). (d) Plot of the normalized UV intensity at 357 nm vs. the volume percent of DMSO in water for compounds 1–4. In the case of **1**, the normalized green curve in fact reflects a modest absolute change of the UV spectra (Fig. S5†). Isosbestic points are indicated by red circles.

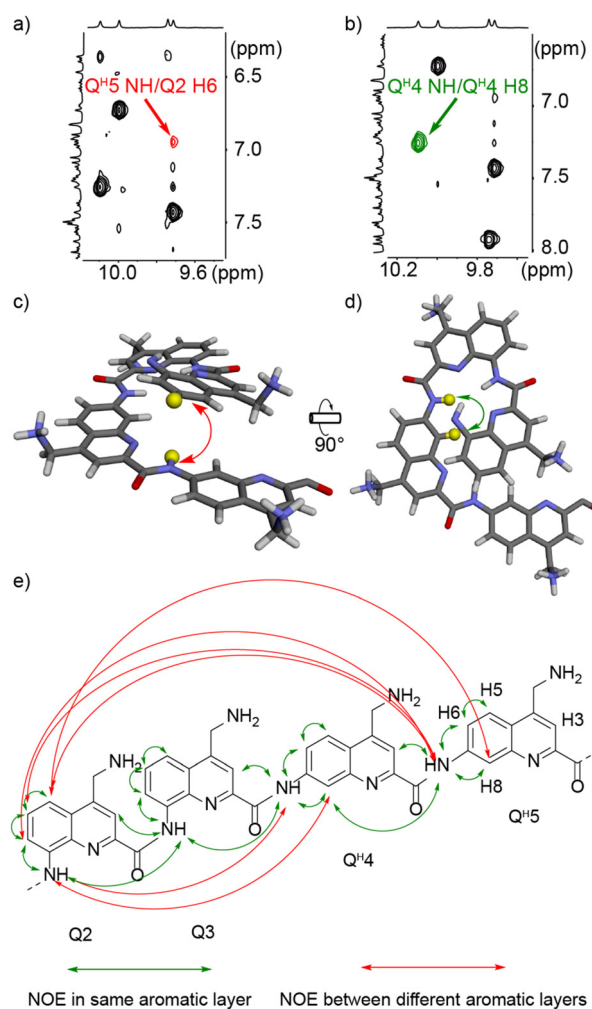


Fig. 5 Selected parts of the ^1H – ^1H NOESY spectrum (500 MHz) of compound 2 showing in (a) the interlayer NOE correlation between Q^H5 NH/ $Q2$ H6 (in red) and in (b) the intralayer NOE correlation between Q^H4 NH/ Q^H4 H8 (in green). Energy minimized models indicating (c) Q^H5 NH/ $Q2$ H6 and (d) Q^H4 NH/ Q^H4 H8 proximity (target protons are highlighted in yellow). (e) NOE interactions observed in the NOESY spectrum of compound 2. All spectra were recorded at 298 K in $\text{H}_2\text{O}/\text{D}_2\text{O}$ (90 : 10 v/v).

carbon, see Fig. 5e for numbering), and NOESY (e.g. correlation of H3 and H5 to the exocyclic CH₂ protons) experiments. NOE correlations between amide NH signals allowed for the assignment of each spin system to its position in the sequence. Finally, the NOESY spectrum revealed multiple correlations between units contiguous in the sequence or stacked above one another that can only arise in a helical structure. Representative examples are shown in Fig. 5. In particular, Q^H units could be shown to adopt the *s-trans* conformation at their position 7 (Fig. 1), which allowed to propose that the structure shown in Fig. 2b is a valid model of the conformation of 2 in water.

Conclusions

In summary, a new flexible monomer Q^H was developed to quickly access water soluble AOF sequences with capsule-like shapes *via* SPS. This monomer promotes a solvent dependence of folding behavior that is uncommon in AOFs. Sharp transitions between unfolded and helically folded states were observed upon adding water to DMSO solutions. Increasing the flexibility of a molecular system is a less common path than the reverse, but the approach has been straightforward because the starting point – the rigid conformations of AOFs – was so well defined. The approach may be extended by using monomers even less helicogenic than Q^H and modulated by combining Q^H with monomers less influenced by solvent such as Q^F. Because of their capsule shape, *i.e.* their larger diameter in the middle of their sequences, molecules 1–4 are potential hosts for molecular recognition. These properties are being investigated and will be reported in due course.

Conflicts of interest

There are no conflicts to declare.

Acknowledgements

This work was supported by the DFG (project HU 1766/6-1). B. Teng gratefully acknowledges financial support from the China Scholarship Council. We thank D. Gill and E. Merlet for contributing some synthetic precursors.

References

- X. Hu, A. Schulz, J. O. Lindner, M. Grüne, D. Bialas and F. Würthner, *Chem. Sci.*, 2021, **12**, 8342–8352.
- J. C. Nelson, J. G. Saven, J. S. Moore and P. G. Wolynes, *Science*, 1997, **277**, 1793–1796.
- H. Goto, H. Katagiri, Y. Furusho and E. Yashima, *J. Am. Chem. Soc.*, 2006, **128**, 7176–7178.
- K. P. de Carvasal, N. Aissaoui, G. Vergoten, G. Bellot, J.-J. Vasseur, M. Smietana and F. Morvan, *Chem. Commun.*, 2021, **57**, 4130–4133.
- H. S. Chan, S. Bromberg, K. A. Dill, C. M. Dobson and A. R. Fersht, *Philos. Trans. R. Soc., B*, 1995, **348**, 61–70.
- Y. Zhao and J. S. Moore, in *Foldamers*, ed. I. Huc and S. Hecht, John Wiley & Sons, Ltd, 2007, pp. 75–108.
- Y. Hua, Y. Liu, C.-H. Chen and A. H. Flood, *J. Am. Chem. Soc.*, 2013, **135**, 14401–14412.
- M. T. Stone, J. M. Heemstra and J. S. Moore, *Acc. Chem. Res.*, 2006, **39**, 11–20.
- K. P. Divya, S. Sreejith, C. H. Suresh, D. S. Phillips and A. Ajayaghosh, *Chem. – Asian J.*, 2013, **8**, 1579–1586.
- K.-J. Chang, B.-N. Kang, M.-H. Lee and K.-S. Jeong, *J. Am. Chem. Soc.*, 2005, **127**, 12214–12215.
- H. Juwarker and K.-S. Jeong, *Chem. Soc. Rev.*, 2010, **39**, 3664–3674.
- V. R. Naidu, M. C. Kim, J. Suk, H.-J. Kim, M. Lee, E. Sim and K.-S. Jeong, *Org. Lett.*, 2008, **10**, 5373–5376.
- E. A. John, C. J. Massena and O. B. Berryman, *Chem. Rev.*, 2020, **120**, 2759–2782.
- C. J. Massena, D. A. Decato and O. B. Berryman, *Angew. Chem., Int. Ed.*, 2018, **57**, 16109–16113.
- S. Peddi, M. C. Bookout, G. N. Vemuri and C. S. Hartley, *J. Org. Chem.*, 2022, **87**, 3686–3690.
- C. S. Hartley, *Acc. Chem. Res.*, 2016, **49**, 646–654.
- H. Jiang, J.-M. Léger and I. Huc, *J. Am. Chem. Soc.*, 2003, **125**, 3448–3449.
- X. Yang, A. L. Brown, M. Furukawa, S. Li, W. E. Gardinier, E. J. Bukowski, F. V. Bright, C. Zheng, X. C. Zeng and B. Gong, *Chem. Commun.*, 2003, 56–57.
- A. M. Abramyan, Z. Liu and V. Pophristic, *Chem. Commun.*, 2015, **52**, 669–672.
- Z. Liu, A. M. Abramyan and V. Pophristic, *New J. Chem.*, 2015, **39**, 3229–3240.
- L. Yuan, H. Zeng, K. Yamato, A. R. Sanford, W. Feng, H. S. Atreya, D. K. Sukumaran, T. Szyperski and B. Gong, *J. Am. Chem. Soc.*, 2004, **126**, 16528–16537.
- J. Wang, B. Wicher, V. Maurizot and I. Huc, *Chem. – Eur. J.*, 2021, **27**, 1031–1038.
- T. Qi, V. Maurizot, H. Noguchi, T. Charoenraks, B. Kauffmann, M. Takafuji, H. Ihara and I. Huc, *Chem. Commun.*, 2012, **48**, 6337–6339.
- J. M. Cary and J. S. Moore, *Org. Lett.*, 2002, **4**, 4663–4666.
- X. Yang, L. Yuan, K. Yamato, A. L. Brown, W. Feng, M. Furukawa, X. C. Zeng and B. Gong, *J. Am. Chem. Soc.*, 2004, **126**, 3148–3162.
- H. H. Nguyen, J. H. McAliley and D. A. Bruce, *Macromolecules*, 2011, **44**, 60–67.
- M. Banno, T. Yamaguchi, K. Nagai, C. Kaiser, S. Hecht and E. Yashima, *J. Am. Chem. Soc.*, 2012, **134**, 8718–8728.
- W. Hu, N. Zhu, W. Tang and D. Zhao, *Org. Lett.*, 2008, **10**, 2669–2672.
- H.-G. Jeon, J. Y. Jung, P. Kang, M.-G. Choi and K.-S. Jeong, *J. Am. Chem. Soc.*, 2016, **138**, 92–95.

- 30 Y. Hua and A. H. Flood, *J. Am. Chem. Soc.*, 2010, **132**, 12838–12840.
- 31 Y. Liu, F. C. Parks, W. Zhao and A. H. Flood, *J. Am. Chem. Soc.*, 2018, **140**, 15477–15486.
- 32 J. Shang, Q. Gan, S. J. Dawson, F. Rosu, H. Jiang, Y. Ferrand and I. Huc, *Org. Lett.*, 2014, **16**, 4992–4995.
- 33 C. Dolain, A. Grélard, M. Laguerre, H. Jiang, V. Maurizot and I. Huc, *Chem. – Eur. J.*, 2005, **11**, 6135–6144.
- 34 *Maestro*, *Schrödinger*, LLC, New York, NY, 2021.
- 35 X. Hu, S. J. Dawson, P. K. Mandal, X. de Hatten, B. Baptiste and I. Huc, *Chem. Sci.*, 2017, **8**, 3741–3749.
- 36 Q. Gan, C. Bao, B. Kauffmann, A. Grélard, J. Xiang, S. Liu, I. Huc and H. Jiang, *Angew. Chem., Int. Ed.*, 2008, **47**, 1715–1718.
- 37 C. Bao, B. Kauffmann, Q. Gan, K. Srinivas, H. Jiang and I. Huc, *Angew. Chem., Int. Ed.*, 2008, **47**, 4153–4156.
- 38 Y. Ferrand and I. Huc, *Acc. Chem. Res.*, 2018, **51**, 970–977.
- 39 W. Wang, C. Zhang, S. Qi, X. Deng, B. Yang, J. Liu and Z. Dong, *J. Org. Chem.*, 2018, **83**, 1898–1902.
- 40 B. Baptiste, C. Douat-Casassus, K. Laxmi-Reddy, F. Godde and I. Huc, *J. Org. Chem.*, 2010, **75**, 7175–7185.
- 41 V. Corvaglia, F. Sanchez, F. S. Menke, C. Douat and I. Huc, *Chem. – Eur. J.*, 2023, DOI: [10.1002/chem.202300898](https://doi.org/10.1002/chem.202300898).
- 42 G. Lautrette, B. Wicher, B. Kauffmann, Y. Ferrand and I. Huc, *J. Am. Chem. Soc.*, 2016, **138**, 10314–10322.
- 43 N. Chandramouli, Y. Ferrand, G. Lautrette, B. Kauffmann, C. D. Mackereth, M. Laguerre, D. Dubreuil and I. Huc, *Nat. Chem.*, 2015, **7**, 334–341.
- 44 D. J. Hill and J. S. Moore, *Proc. Natl. Acad. Sci. U. S. A.*, 2002, **99**, 5053–5057.
- 45 R. B. Prince, J. G. Saven, P. G. Wolynes and J. S. Moore, *J. Am. Chem. Soc.*, 1999, **121**, 3114–3121.